

Relativistic tunneling picture of electron-positron pair creation

Anton Wöller^{*}, Michael Klaiber, Heiko Bauke[†] and Christoph H. Keitel
 Max-Planck-Institut für Kernphysik, Saupfercheckweg 1, 69117 Heidelberg, Germany
 (Dated: March 20, 2015)

The common tunneling picture of electron-positron pair creation in a strong electric field is generalized to pair creation in combined crossed electric and magnetic fields. This enhanced picture, being symmetric for electrons and positrons, is formulated in a gauge-invariant and Lorentz-invariant manner for quasistatic fields. It may be used to infer qualitative features of the pair creation process. In particular, it allows for an intuitive interpretation of how the presence of a magnetic field modifies and, in particular cases, even enhances pair creation. The creation of electrons and positrons from the vacuum may be assisted by an energetic photon, which can also be incorporated into this picture of pair creation.

PACS numbers: 12.20.Ds, 42.55.Vc, 42.50.Hz

1. Introduction and motivation

One of the most intriguing predictions of quantum electrodynamics (QED) is certainly the possible breakdown of the vacuum in the presence of ultrastrong electromagnetic fields into pairs of electrons and positrons. Since its first prediction by Sauter and others [1–4], pair creation has been studied in many papers, see Refs. [5–7] for recent reviews. The Schwinger critical field strength of $E_S = 1.3 \times 10^{18}$ V/m, where spontaneous pair creation is expected to set in, cannot be reached even by the strongest lasers available today. However, pair creation may be assisted by additional fields or particles. Current research covers, among others, pair creation in spatially and temporally oscillating electric fields [8–11], pair creation induced by the interaction of strong pulsed laser fields with relativistic electron beams or a nuclear Coulomb field (Bethe-Heitler process) [12–15], and pair creation induced by additional photons in the presence of an external field [16–20]. Furthermore, different aspects of pair creation like the effect of magnetic fields [21–23], the dynamics, real-time evolution and pair distributions with nontrivial field configurations in one effective dimension [24–28], and effective mass signatures in multiphoton pair creation [29] are investigated at present. Current interest in the old topic of pair creation is prompted by recent advances in laser technology [30, 31] aiming for laser intensities exceeding 10^{22} W/cm² (corresponding to electric field strengths of about 10^{14} V/m) and by experimental proposals for quantum simulators [32] that may allow to study pair creation via quantum simulation. The ultimate quest for higher and higher laser intensities for studying quantum electrodynamic effects such as pair creation may be limited, however, just by the onset of pair creation [33].

At field strengths below the Schwinger limit E_S , pair creation via ultrastrong electric fields may be interpreted as a tunneling effect [34] similar to tunnel ionization from bound states via strong electric fields [35, 36] using the method of imaginary times [37] (see also recent applications in Refs. [38–40]). This method uses classical trajectories with imaginary

times to approximate the exponential suppression for the transition amplitude of interest. In spite of conceptual difficulties [41, 42], the tunneling picture of ionization was recently extended into the relativistic domain, where the laser’s magnetic field component can no longer be neglected [43, 44]. The purpose of this contribution is to establish a similar picture for pair creation in an electromagnetic field, including the magnetic field to full extent. The influence of an additional quantized photon is incorporated and special care is taken with respect to gauge and Lorentz invariance. The tunneling picture presented here is established in the quasistatic limit, where the electromagnetic field is assumed to be constant and uniform during the pair creation process. Furthermore, spin effects are not taken into account.

The manuscript is organized as follows: In Sec. 2 we describe the electromagnetic field configuration for pair creation, lay down the theoretical framework, and introduce all necessary notations. Our main results are presented in Sec. 3, where the tunneling picture for electron-positron pair creation in quasistatic crossed electric and magnetic fields is developed. Three different cases need to be distinguished, depending on the electric field amplitude being larger than, equal to, or smaller than the magnetic field amplitude. The effect of a quantized photon is also discussed for all these cases. Properties of the maximum probability trajectories, stemming from the imaginary time method, are investigated in Sec. 4. Finally, we conclude in Sec. 5. Further details of the calculations have been deferred into two appendices.

2. Theoretical framework

2.1. Geometric setup and notation

Natural units will be used in this work, i. e., $c = \hbar = 1$. The setup of the considered pair production process in an electromagnetic field of an ultrastrong laser is depicted in Fig. 1. The electric field with amplitude E points in the x direction, and the magnetic field with amplitude B in the y direction. This configuration corresponds to the quasistatic limit of either a plane-wave field or two counterpropagating laser fields. In the

^{*} woeller@mpi-hd.mpg.de

[†] heiko.bauke@mpi-hd.mpg.de

case of a plane-wave field, its wave vector will be directed along the positive z direction, and the amplitudes of the electric and magnetic fields will be equal. The superposition of two counterpropagating laser fields can lead to orthogonal electric and magnetic fields of different magnitudes. Note that the orthogonality of the considered setup is maintained under Lorentz boosts because $\mathbf{E} \cdot \mathbf{B} = 0$ is Lorentz invariant. Furthermore, because $\mathbf{B}^2 - \mathbf{E}^2$ is invariant under Lorentz boosts, the relative strength of the electric and magnetic fields is also maintained. This will lead us later to the distinction between the cases $|E| > |B|$, $|E| = |B|$, and $|E| < |B|$. Note that for $|E| > |B|$, one can always boost along the z direction into a new reference frame where $B' = 0$. Similarly for $|E| < |B|$, there exists a reference frame where $E' = 0$. For $|E| = |B|$, all boosts along the z direction maintain the condition $|E'| = |B'|$.

The wave vector of a possibly assisting high-energy photon is parallel to the z direction; i. e., it may be positive or negative. Other relative orientations of the photon and the electromagnetic field are not considered here because such a setup would lead to a reduced or even vanishing pair production rate.

In the following sections, we will utilize a semiclassical description of pair creation based on classical trajectories. For an economical description of these trajectories, the following notation will be used: The electron's kinetic four-momentum is written as

$$p^\mu = (p_0, p_x, p_y, p_z), \quad (1)$$

and likewise its canonical momentum P^μ . The kinetic and canonical momentum of the positron are denoted by q^μ and Q^μ , respectively. The wave vector for the photon k^μ is written, according to the geometry used in this work, as

$$k^\mu = (k_0, 0, 0, k_z) \quad (2)$$

with $k_0 = |k_z|$. As the motion of the particles can be reduced to a one-dimensional description along the x direction, we denote the electron's and positron's x coordinates by x^- and x^+ (not to be confused with light-cone coordinates). Variables and their

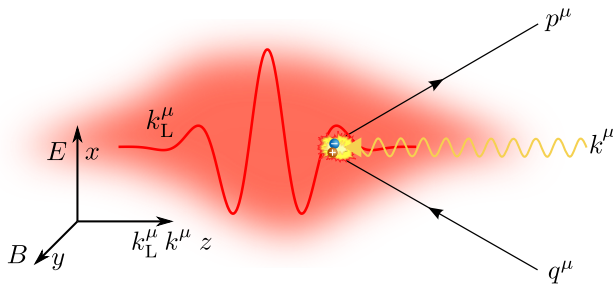


FIG. 1: (color online) Schematic illustration, representing the geometry of the physical setup. An electron and a positron with the kinetic four-momenta p^μ and q^μ are created in the presence of a strong external electromagnetic field (red shading), e. g., a plane wave or two colliding laser pulses. Pair production may be assisted by an additional high-energy photon with four-momentum k^μ (yellow). The directions of the electric field, the magnetic field, and the photon momentum are perpendicular to each other and parallel to the coordinate axes.

values at the point of pair production x_s will be subindexed by “s”, thus $p_s^\mu = p^\mu(x_s)$ or x_s^- being the x component of the electron's position at x_s . Variables and their values at the point where the electron or the positron leave the imaginary trajectory will be subindexed by “e” (for exit), thus $p_{x,e} = p_x(x_e^-)$ being the kinetic momentum of the electron in the x direction at its point of exit.

The equations of motion for the canonical momenta of the electron and the positron with charge $\mp e$ are given by

$$\frac{d}{dt} P^\mu = -e \frac{\partial x^\nu}{\partial t} \frac{\partial A_\nu}{\partial x_\mu}, \quad (3a)$$

$$\frac{d}{dt} Q^\mu = e \frac{\partial x^\nu}{\partial t} \frac{\partial A_\nu}{\partial x_\mu}, \quad (3b)$$

where A_ν denotes the electromagnetic field's four-potential. The electron's and the positron's kinetic and canonical momenta are connected via

$$p^\mu(x) = P^\mu(x) + eA^\mu(x), \quad (4a)$$

$$q^\mu(x) = Q^\mu(x) - eA^\mu(x). \quad (4b)$$

2.2. Matrix elements for pair creation

The mathematical handle for pair production is given by its so-called matrix element or transition amplitude from an initial vacuum state (possibly including a photon) to a final state with an electron and positron (see Ref. [45] for a thorough treatment). For an external electromagnetic field only, this is given by

$$M_{fi} = \langle 1_p, 1_q, \text{out} | 0, \text{in} \rangle. \quad (5a)$$

Both the initial in-state and the final out-state are defined in the Furry picture [46] and refer to a common time (see also Appendix A or Ref. [45]). The asymptotic four-momenta of the electron and positron are indicated by p and q .

In the case of an additional quantized photon field, which may assist the process, the matrix element will read in first-order perturbation theory

$$M_{fi} = i \int dx \langle 1_p, 1_q, \text{out} | \hat{\mathcal{H}}_{\text{int}}(x) | 1_k, \text{in} \rangle. \quad (5b)$$

The four-momentum of the quantized photon is labeled by k , and $\hat{\mathcal{H}}_{\text{int}}$ designates the QED interaction vertex. Using semiclassical methods, the exponential parts of both matrix elements can be evaluated approximately. Here, semiclassical refers to the fact that only classical trajectories (although possibly imaginary) connecting the in- and the out-states are taken into account in the path-integral picture. As shown in Appendix A (see Eqs. (A32) and (A41)), this approximation yields

$$M_{fi} \sim \exp \left[-\text{Im} (W_k + W_p + W_q) \right]. \quad (6)$$

W_p and W_q are the gauge-dependent classical actions of the electron and positron with asymptotic momentum p and q in

the external field. Likewise, W_k gives the classical action of the quantized photon with momentum k . Note that both transitions (with or without an additional high-energy photon) may coexist. The limit $k \rightarrow 0$ leads to a vanishing amplitude in Eq. (5b) due to prefactors, but the exponential approaches the same value as the exponential in Eq. (5a). Therefore, in the case of no additional photon, W_k in Eq. (6) is set to zero. The various actions in (6) are not the same as the commonly used actions $S(x', x)$, which connect a position eigenstate with another position eigenstate. Rather, they are Legendre transforms thereof, connecting a position eigenstate with a momentum eigenstate (x' being implicitly defined by the canonical momenta, see Appendix A):

$$W_p(x) = S_p(x', x) - \mathbf{P} \cdot \mathbf{x}', \quad (7a)$$

$$W_q(x) = S_q(x', x) - \mathbf{Q} \cdot \mathbf{x}', \quad (7b)$$

$$W_k(x) = S_k(x, x') + \mathbf{K} \cdot \mathbf{x}'. \quad (7c)$$

The classical trajectories will consist of a path of the incoming photon toward the point of pair creation x_s , where the photon converts into an electron and positron, and two outgoing paths of the created particles from x_s onward. If there is no photon, the pair is created out of the vacuum at x_s . The exponent of Eq. (6) is therefore the imaginary part of the action, acquired by a photon coming from the past and propagating with momentum k to x_s , and the two actions, acquired by the electron and positron propagating from x_s to the future with momenta p and q . Although the classical actions are gauge dependent, the square modulus of Eq. (6) is not, as the boundary terms at x_s cancel each other and the boundary terms at $\pm\infty$ result in unimportant phases. Due to the Lorentz invariance of the actions, Eq. (6) is also invariant under Lorentz transformations.

2.3. Kinetic considerations at the point of pair production

At the point of pair production x_s^μ , the classical energy-momentum conservation

$$p_s^\mu + q_s^\mu = k^\mu \quad (8)$$

must be satisfied for the trajectory being classical. This cannot happen on real classical trajectories, but on imaginary ones. Squaring both sides of $k^\mu - p_s^\mu = q_s^\mu$ leads to

$$kp_s = 0 = k_0 p_{0,s} - k_z p_{z,s}, \quad (9)$$

yielding with $k_0 = |k_z|$

$$p_{0,s}^2 = p_{z,s}^2, \quad (10)$$

and likewise for q_s^μ . Hence, using the relativistic dispersion relation and squaring p_s and q_s gives

$$m^2 = -p_{x,s}^2 - p_{y,s}^2 = -q_{x,s}^2 - q_{y,s}^2. \quad (11)$$

Due to the fact that p_y and q_y are constants of motion in the aforementioned setup, they have to be real to be consistent with

a real asymptotic momentum. Therefore, $p_{x,s}$ and $q_{x,s}$ must be purely imaginary:

$$p_{x,s} = -q_{x,s} = \pm i \sqrt{m^2 + p_y^2} = \pm i m_*, \quad (12)$$

$$m_* \equiv \sqrt{m^2 + p_y^2}. \quad (13)$$

Starting from x_s , both the trajectory of the electron and the trajectory of the positron need to be followed until the exit points in order to calculate the imaginary part of the action along these trajectories. The trajectories will be called “imaginary”, as long as the momenta p_x and q_x are still imaginary. Hence, the exit points are given by the condition that p_x and q_x become zero, and consequently, real:

$$p_{x,e} = 0 = q_{x,e}. \quad (14)$$

3. Tunneling picture for the constant field approximation

The tunneling picture, presented in this work, is based on the assumption that the external electromagnetic field can be treated as constant and uniform during the imaginary part of the trajectory. In Sec. 3.1 this assumption will be discussed in more detail, and the kinetic equations necessary for determining the pair creation probability will be derived. Based on these findings, an intuitive picture of pair creation will be derived in Sec. 3.2 and discussed in detail in the remaining subsections. In order to establish this enhanced picture it is necessary to study the semiclassical trajectories during pair creation in detail.

3.1. Kinetics within the constant field approximation

Expanding the electromagnetic field in the region of interest just up to linear terms in x^μ leads to a constant and uniform electric and magnetic field. For the case of an external field due to two counterpropagating lasers, the approximation is justified if the spacetime region of the imaginary dynamics, which is $|x_s^\mu - x_e^\mu|$, is small compared to the spacetime region on which the electromagnetic field varies. In the case of an external plane-wave field, this approximation is also valid if the imaginary trajectory is such that both the electron and the positron move closely to the plane wave’s phase and therefore see the same field everywhere. Hence, applying the constant field approximation requires us to check, after calculating the trajectories, that along these, the electromagnetic field under consideration can really be treated as constant. In general, the electromagnetic field is evaluated at complex spacetimes. Using the constant field approximation, the vector potential for the electromagnetic field may be written as

$$A_\mu(t, z) = (0, Et - Bz, 0, 0). \quad (15)$$

Here, E and B correspond to the values of the electric and magnetic fields at the point where the electromagnetic field is

expanded. For crossed or counterpropagating laser beams, it might be possible that $|E| \neq |B|$. Thus allowing for arbitrary values of E and B , there are three different cases: $|E| > |B|$, $|E| = |B|$, and $|E| < |B|$. The corresponding Lorentz-invariant quantity

$$\mathcal{E} \equiv \sqrt{|E|^2 - B^2} \quad (16)$$

will also be used in this work.

Integrating the equations of motion (3) with constant crossed fields of the geometry in Fig. 1 yields

$$p_0(x^-) = p_{0,e} - eE(x^- - x_e^-), \quad (17a)$$

$$p_z(x^-) = p_{z,e} - eB(x^- - x_e^-), \quad (17b)$$

$$q_0(x^+) = q_{0,e} + eE(x^+ - x_e^+), \quad (17c)$$

$$q_z(x^+) = q_{z,e} + eB(x^+ - x_e^+). \quad (17d)$$

Thus, both the kinetic energy and the z momentum depend only linearly on the position in the x direction, simplifying the calculation considerably. In contrast to Schwinger pair creation with an electric field only, the electron and the positron will be accelerated along the z direction in the presence of a magnetic field, see Eqs. (17b) and (17d). Furthermore, the magnetic field guides both particles in the same direction, while the electric field accelerates the particles into opposite directions. The x dependence for p_x and q_x is given implicitly by the dispersion relation $p^2 = m^2$:

$$p_x^2(x^-) = p_0^2(x^-) - (m^2 + p_z^2(x^-)), \quad (18a)$$

$$q_x^2(x^+) = q_0^2(x^+) - (m^2 + q_z^2(x^+)). \quad (18b)$$

Using Eq. (17) and the relation from Eq. (9), the length of the imaginary trajectory from x_s to x_e along the x direction for both the electron and the positron is determined by

$$x_s^- - x_e^- = \frac{k_0 p_{0,e} - k_z p_{z,e}}{e(Ek_0 - Bk_z)}, \quad (19a)$$

$$x_e^+ - x_s^+ = \frac{k_0 q_{0,e} - k_z q_{z,e}}{e(Ek_0 - Bk_z)}. \quad (19b)$$

Plugging Eq. (17) into Eq. (8) gives the relations

$$eE(x_e^+ - x_e^-) = p_{0,e} + q_{0,e} - k_0, \quad (20a)$$

$$eB(x_e^+ - x_e^-) = p_{z,e} + q_{z,e} - k_z. \quad (20b)$$

Multiplying (20a) with B , (20b) with E , and subtracting both yields

$$B(p_{0,e} + q_{0,e} - k_0) = E(p_{z,e} + q_{z,e} - k_z). \quad (21)$$

This equation gives the relation between p_e^μ , q_e^μ , and k^μ , as they are not independent of each other.

As a consequence of Eqs. (17) and (18), the kinetic momenta of the particles depend only on the x direction of space. Furthermore, it turns out that the imaginary part of the exponent is solely determined by the momenta in the x direction [47] via

$$W = \int_{x_e^-}^{x_s^-} p_x dx + \int_{x_s^+}^{x_e^+} q_x dx = W^- + W^+, \quad (22)$$

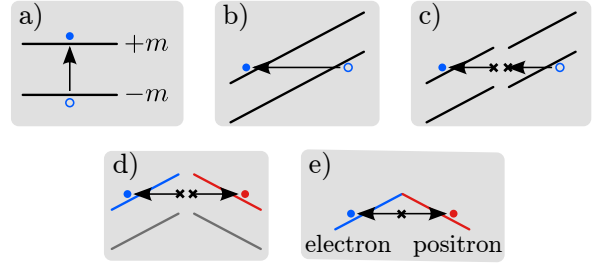


FIG. 2: (color online) The conventional tunneling picture of pair creation as tunneling from the Dirac sea (a) without electric field and (b) with electric field. The tunneling path may be split into two parts (c), which may be interpreted as an electron and a positron emerging in the barrier and tunneling to real positive-energy states (d and e).

although the particles' (imaginary) dynamics can be three-dimensional. The imaginary part is made up from a part due to the electron moving between x_s and x_e^- , where p_x is imaginary, and a part due to the positron moving between x_s and x_e^+ , where q_x is imaginary. The photon's action cancels with the electron's and the positron's actions along the z and t directions due to energy and momentum conservation. The photon will, however, influence the whole dynamics, and in this way the momenta p_x and q_x . The integrals for the exponent Eq. (22) can be calculated analytically using Eq. (18) for the momenta p_x and q_x and (19) for the integration limits. Note that W^+ and W^- are not independent of each other due to momentum conservation at the point of pair creation, see Eq. (8).

3.2. Graphical interpretation of the relativistic tunneling picture

Pair creation in strong electric fields is commonly interpreted as tunneling from a negative-energy state in the Dirac sea to a positive-energy state [34]. In other words, the creation of an electron-positron pair is described by a transition from a one-particle state to another particle state. This picture can, however, be translated into a picture where tunneling starts under the tunneling barrier and the final state after tunneling is a classical two-particle state, see Fig. 2. Although both interpretations are equivalent, a pair creation picture that involves two particles may be more intuitive. In the following, a pair creation picture will be introduced that goes beyond the standard tunneling picture of Ref. [34] by incorporating also an external magnetic field and possibly a high-energy photon. This picture is inspired by the tunneling picture for atomic ionization.

The standard tunneling picture for atomic ionization gives an intuitive measure for the suppression of ionization by means of an area that is determined by the potential function and the particle's energy. If the potential is increased, for example, this area gets larger, thus indicating a reduced tunneling probability. In the same way, the enhanced tunneling picture of pair creation presented in this work will give a measure for the suppression of pair production by means of an area. The exact exponents

are given by the integrals in Eq. (22), which can be pictured by areas given by the integrals of

$$\text{Im } p_x(x) = \sqrt{m_*^2 + p_z^2(x) - p_0^2(x)}, \quad (23a)$$

$$\text{Im } q_x(x) = \sqrt{m_*^2 + q_z^2(x) - q_0^2(x)} \quad (23b)$$

along the x direction. Plotting these quantities directly would yield the exact phase-space areas of the tunneling trajectories, but unfortunately, it does not give any intuitive account on how the pair production changes if, for example, the electric or magnetic field amplitude or the energy of the additional photon changes. However, it will be sufficient to use quantities that are monotonically correlated to the momenta in Eq. (23). These quantities will be called \tilde{p}_x and \tilde{q}_x and will increase or decrease if p_x and q_x increase or decrease. This monotonic correlation assures that the areas spanned by \tilde{p}_x and \tilde{q}_x along the x direction also increase or decrease if the exponents in Eq. (22) increase or decrease. Although the choice for \tilde{p}_x and \tilde{q}_x is not unique, we defined them as

$$\begin{aligned} \text{Im } \tilde{p}_x &= \left| \sqrt{m^2 + p_x^2 + p_y^2 + p_z^2} - \sqrt{m^2 + p_y^2 + p_z^2} \right| \\ &= |p_0 - \tilde{p}_0| = \tilde{p}_0 - p_0, \end{aligned} \quad (24a)$$

$$\begin{aligned} \text{Im } \tilde{q}_x &= \left| \sqrt{m^2 + q_x^2 + q_y^2 + q_z^2} - \sqrt{m^2 + q_y^2 + q_z^2} \right| \\ &= |q_0 - \tilde{q}_0| = \tilde{q}_0 - q_0, \end{aligned} \quad (24b)$$

with the pseudoenergies \tilde{p}_0 and \tilde{q}_0 defined as

$$\tilde{p}_0(x) = \sqrt{m^2 + p_y^2 + p_z^2(x)} = \sqrt{m_*^2 + p_z^2(x)}, \quad (25a)$$

$$\tilde{q}_0(x) = \sqrt{m^2 + q_y^2 + q_z^2(x)} = \sqrt{m_*^2 + q_z^2(x)}. \quad (25b)$$

The areas spanned by \tilde{p}_x and \tilde{q}_x along the x direction are the areas enclosed by the curves of the kinetic energy and the pseudoenergy, both amenable for an intuitive interpretation. The monotonic correlation between the imaginary part of \tilde{p}_x and p_x can be shown by taking the derivative of \tilde{p}_x with respect to p_x , which is always positive. This holds similarly for the monotonic correlation between the imaginary part of \tilde{q}_x and q_x . Furthermore, \tilde{p}_x and \tilde{q}_x are zero if p_x and q_x are zero, which corresponds to the exit points, and hence the exit points are automatically given by the points of intersection between the kinetic and pseudoenergy curves. Despite the fact that this approximation to the area of the exponents is not exact, it is sufficient to derive qualitative results and gives more intuition, as we will show in the following.

The now-introduced quantities can be presented graphically as a function of the x coordinate giving a visual representation of the tunneling picture of pair creation, as shown exemplarily in Fig. 3. The upper black solid line represents the zero-energy reference. Lines for the electron are drawn in blue, whereas lines for the positron are drawn in red. The bold solid colored lines represent the particles' pseudoenergies in Eq. (25) as a function of the particles' real x coordinate and the imaginary z coordinate. The motion into the imaginary z direction results from a real z momentum due to the presence of a magnetic field

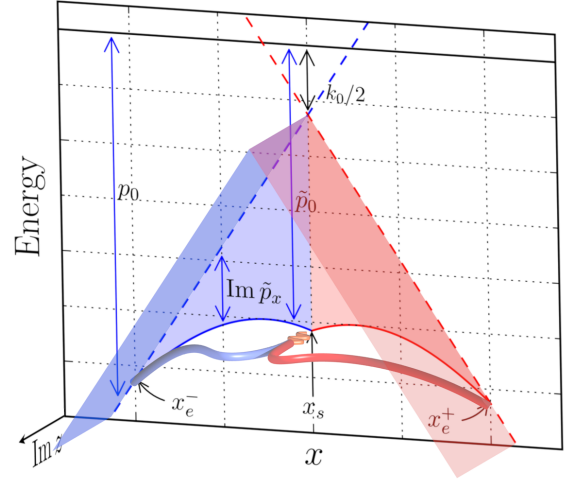


FIG. 3: (color online) The tunneling picture of pair creation, indicating also the quantities used in the text. The electron and the positron start their imaginary trajectory at x_s and travel to their respective exits x_e^- and x_e^+ , where the trajectories become real. The tunneling dynamics is along the real x axis and the presence of a magnetic field may cause a nontrivial motion along the imaginary z axis. The bold solid lines represent the pseudoenergies in Eq. (25) as a function of the x and z coordinates, whereas the thin solid lines indicate the projection of Eq. (25) along the x axis. The dashed lines represent the kinetic energy. The values of the acquired imaginary actions W^- for the electron and W^+ for the positron along these paths determine the exponential term suppressing pair production and can be inferred qualitatively by the shaded areas, enclosed by the thin solid and dashed red and blue lines.

or the initial momentum transfer due to the additional photon during an imaginary time interval. Note, however, that there is no motion in the z direction in real space because tunneling is instantaneous in real time [43]. Because the semiclassical tunneling trajectories do not represent realistic particle paths, the exit coordinate, which is where the particles' momenta become real, is not necessarily real, i.e., $\text{Im } z_e^\pm \neq 0$. This may be related to the fact that each semiclassical trajectory corresponds to a delocalized quantum state with a well-defined momentum, which is given by the exit momentum of the semiclassical trajectory. A real motion into the z direction would require an inhomogeneous electromagnetic field similarly to the near-threshold-tunneling regime of relativistic tunnel ionization [44].

The particles' pseudoenergies in Eq. (25) as well as their kinetic energies in Eqs. (17a) and (17c) can be expressed as functions of the x coordinate only and are represented in Fig. 3 by the solid and dashed lines, respectively. The solid colored lines originate for both the electron and the positron from the initial point for pair creation x_s and end at their respective exit points x_e^- and x_e^+ , where they intersect the dashed lines. Hence, by following, for example, the blue dashed and solid lines, the change in kinetic energy and pseudoenergy can be traced along the x direction of the imaginary trajectory from the point of pair creation until the exit for the electron, and

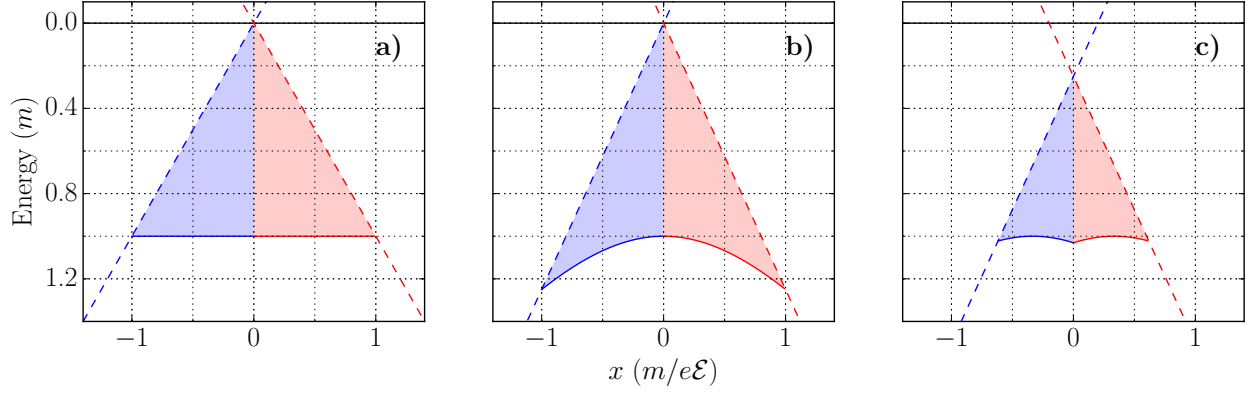


FIG. 4: (color online) The tunneling picture of pair creation for $|E| > |B|$. (a) The standard Schwinger case with an electric field only is considered. (b) An inertial system, which is Lorentz-boosted relatively to that of (a) along the z direction with $v/c = -3/5$ leading to a nonzero magnetic field. The larger (boosted) electric field leads to a steeper increase of the kinetic energy (dashed line). Furthermore, the magnetic field increases the pseudoenergy (solid lines) due to the buildup of momentum along the z direction. (c) The same configuration as in part (b), but with an additional photon of momentum $k_0 = m/2$. Its kinetic energy is shared by the created electron and positron, shifting their kinetic energies (dashed lines) down by $k_0/2$ and in this way decreasing the shaded area. Also, the kinetic momentum of the photon is shared by the produced electron and the positron shifting the initial pseudoenergy (solid lines) at x_s downwards.

similarly for the positron by following the red lines. Finally, a blue shaded area for the electron and a red shaded area for the positron are shown, which are enclosed by the dashed and solid colored lines. These areas can be related to exponents for pair production.

After introducing the different constituents of the enhanced tunneling picture, their physical interpretation can be explained now. At the point of pair creation x_s , the sum of the kinetic energies of the electron and the positron must be equal to the initial energy already existing in the system. This is either zero or k_0 in the case of an additional photon. From x_s , both the electron and the positron follow their imaginary trajectories until their respective exits. The trajectories will be imaginary as long as p_x and q_x are imaginary or equivalently as long as the pseudoenergies \tilde{p}_0 and \tilde{q}_0 are larger than their respective kinetic energies p_0 and q_0 . In the graphs this can be seen by the solid colored lines lying below the dashed colored lines. At the exits, $p_x = 0$ and $q_x = 0$, both lines intersect as both types of energy (pseudo and kinetic) become equal. Note that the kinetic energies go below their minimum allowed energy behind the exit points towards x_s , where p_x and q_x get imaginary. It is just this behavior that allows the fulfillment of Eq. (8), i.e., energy-momentum conservation at x_s . Furthermore, the difference between the pseudoenergy and kinetic energy is taken as an approximate measure for the imaginary part of the particles' x momenta, see Eq. (24). The exponent for pair production, Eq. (22), is given by the integral over p_x and q_x along the x direction from the point of pair creation x_s to both the exit points of the electron and positron. Hence, the absolute value of these exponents can be inferred approximately by the shaded areas in the graphs. Thus, the shaded blue area corresponds to W^- and the shaded red area corresponds to W^+ . In the following three subsections, the qualitative behavior of these shaded areas—that is, the pair production exponent—will be discussed depending on different factors like the ratio of electric and magnetic field strength or the impact of an additional

photon.

3.3. Case $|E| > |B|$

Figure 4 shows some common cases where the electric field is stronger in magnitude than the magnetic field. It can be readily seen that for these cases, pair production is always possible due to the existence of the exit points, given by the intersection of the dashed and solid lines. For $|E| > |B|$, this intersection is always possible, because the pseudoenergy line (solid) never falls more steeply than the kinetic energy line (dashed), and hence, they need to intersect somewhere.

In Fig. 4(a), Schwinger pair creation is considered with an electric field only and without an additional photon. Furthermore, the most probable case with zero momentum at the exit is taken. The pseudoenergies \tilde{p}_0 and \tilde{q}_0 (the solid colored lines) are constant, because p_z and q_z do not change when there is no magnetic field, and p_y as well as q_y are constants of motion. At x_s , both kinetic energies of the electron and the positron are zero in sum, as there is no additional energy without a photon. The Lorentz-boosted version of Fig. 4(a), seen in a reference frame boosted along the z direction, is shown in Fig. 4(b). Due to the boost, the electric field gets larger, and hence the dashed colored lines get steeper. The stronger electric field alone would increase the tunneling probability. But due to the boost, a magnetic field is also experienced now by the particles, which transfers momentum from the x direction to the z direction. This momentum transfer reduces the acceleration into the electric field direction and makes pair creation less probable. In the tunneling picture, the momentum transfer is represented by the bent pseudoenergies \tilde{p}_0 and \tilde{q}_0 ; see Fig. 4(b). Furthermore, the energy of the created particles is increased, which is consistent with the boost in the z direction. The growth of the relativistic mass is seen by the bending of the pseudoenergy

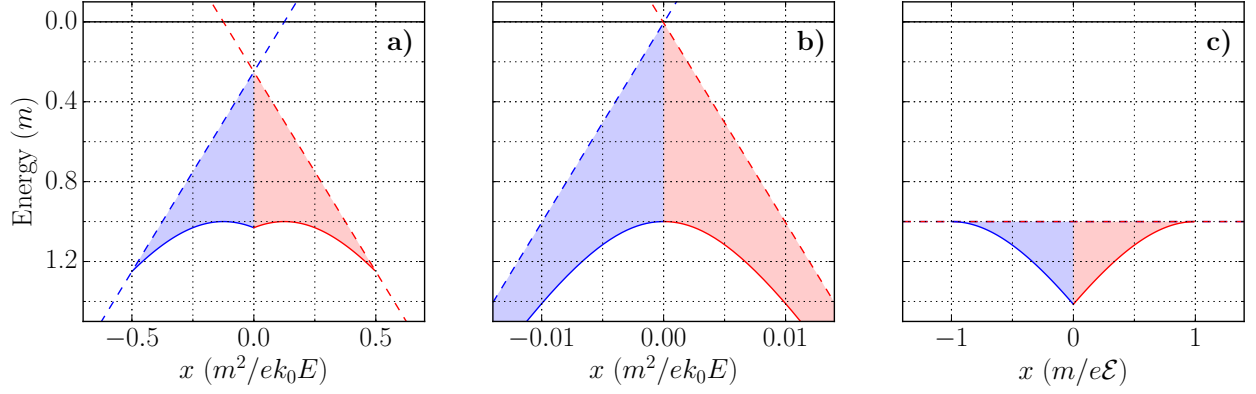


FIG. 5: (color online) Part (a) and (b) show the tunneling picture for the plane-wave case $|E| = |B|$, with an additional photon with $k_0 = m/2$ and $k_0 = m/100$, respectively, similarly to Fig. 4(c). In this case, an additional photon propagating opposite to the external electric field is needed for pair creation. Without this photon, the solid and dashed lines become tangent asymptotically, yielding an infinite area and hence no pair production. From a kinetic point of view, the magnetic field (being as strong as the electric field) builds up as much z momentum (increasing the pseudoenergy) as the electric field kinetic energy, and hence the particles cannot become real. The energy shift by the photon is enough to let both lines intersect each other, provided that its z momentum is opposite to the buildup due to the magnetic field. The case with a magnetic field only is shown in part (c). To render pair production possible, the incoming photon must have at least 2 times the rest mass energy, i. e., $k_0 \geq 2m$, because the magnetic field only cannot transfer energy. It can be seen from the diagram that the initial z momentum, transferred from the photon to the electron and positron, is rotated along the imaginary trajectory onto the x momentum and hence reduces the initial imaginary x momentum to zero at the exits, making the electron and positron real, and therefore pair production possible.

lines. Both effects, the increase of the electric field and the increase of the relativistic energy, cancel each other exactly, as the transition amplitude is Lorentz invariant. This invariance is also represented in Figs. 4(a) and 4(b), since the size of the shaded areas remains almost constant under the Lorentz boost, although the areas are a qualitative measure for the tunneling probability. Note also that the x coordinate of the exit points x_e^- and x_e^+ does not change, as it is not affected by a boost along the z direction. Furthermore, Fig. 4(b) allows us to infer the effect of a magnetic field that is superimposed to a given electric field. The area in Fig. 4(b) is increased due to the bending of the solid lines opposed to the case without magnetic field, where these lines are horizontal. Consequently, the pair production rate is decreased.

In Fig. 4(c), an additional photon is incorporated into the setting of E and B in Fig. 4(b). Here, two very important things can be seen immediately. First, the additional energy of k_0 at x_s . Both the electron and the positron can now share this energy, which is $k_0/2$ per particle for maximum pair production probability. For this reason, the dashed colored lines are shifted down by $k_0/2$. This decreases the shaded areas and therefore increases the pair production probability. Secondly, the additional photon does not only transfer its kinetic energy; it also transfers its momentum along the z direction. This leads to an additional z momentum of $k_0/2$ for both the electron and the positron, increasing their pseudoenergy, or equivalently, their relativistic mass at x_s . Without a magnetic field, this extra energy due to the z momentum remains until the exit and must be supported by the electric field, ultimately decreasing the pair production probability due to a longer “time” until the exit. To summarize, the additional photon transfers energy, which enhances the probability, but it also transfers momentum, which degrades the probability. In total, this results always in an

enhanced probability. The degradation due to the momentum transfer along the z direction can be reduced by tuning the magnetic field in such a way that it decelerates the particles along the z direction, thus making them “lighter” at the exits. The appropriate tuning of the magnetic field will be discussed in more detail in Sec. 4. From Eq. (20) it can be shown that the direction in which the electron and the positron are accelerated along the x direction is determined only by the orientation of the electric field,

$$\text{sgn}(x_e^+ - x_e^-) = \text{sgn } E. \quad (26)$$

This is represented in the tunneling picture by the slope of the kinetic energy lines being positive or negative, forcing the particles in the one or the other direction.

Calculating the tunneling probability via the integral in Eq. (22) gives for the electron

$$W^- = i \frac{(Ep_{0,e} - Bp_{z,e})^2}{2\mathcal{E}^3} (\arccos \Gamma - \Gamma \sqrt{1 - \Gamma^2}) \quad (27)$$

with

$$\Gamma = 1 - e \frac{E^2 - B^2}{Ep_{0,e} - Bp_{z,e}} (x_s^- - x_e^-). \quad (28)$$

The quantity W^+ has the same analytical structure, but the momenta and the position of the electron need to be replaced by that of the positron. For the standard Schwinger case, which is just an electric field without an additional photon and with zero momentum at the exit, W^- in Eq. (27) reduces to $i\pi m^2/(4E)$. Adding W^+ and multiplying by 2, which corresponds to the square modulus of the matrix element, gives exactly the Schwinger exponent $\pi m^2/E$. Furthermore, if the

electrical field strength E is replaced by its corresponding Lorentz invariant \mathcal{E} , then this result also agrees with the first-order exponent in the work [48] for nonzero magnetic fields in the case of no additional photon.

3.4. Case $|E| = |B|$

This case is somewhat special, because it connects the previous and the next case in a singular manner. It corresponds to an external plane-wave field under the constant crossed field approximation. Figures 5(a) and 5(b) show the tunneling picture for a quantized photon of energy $k_0 = m/2$ and $k_0 = m/100$. In general, the picture is quite similar to that of Fig. 4(c), but here a quantized photon is mandatory for pair production. Due to the magnetic field being as strong as the electric field, the energy transferred to the particles in z momentum by the magnetic field is as strong as the kinetic energy transferred to the particles by the electric field. In this sense, the electric field without an additional photon is not strong enough to let the particles leave the imaginary trajectories, as the magnetic field makes them more and more heavy. This can be seen by comparing in Figs. 5(a) and 5(b) how the colored dashed and solid lines approach each other. In the limit of k going to zero, the kinetic and pseudoenergy lines become tangent and will not intersect, leading to an infinite exponent and thus no pair production.

Depending on the orientation of E and B , which is connected with the orientation of k_L for a plane wave ($E \times B$ points into the same direction as k_L), the quantized photon has to be directed antiparallel to the external field wave vector. In the given geometry, this means that

$$\text{sgn } k_z = -\text{sgn } (EB) \quad (29)$$

has to be satisfied. Otherwise, there will be no pair production, as the quantized photon and external field will be parallel, which can be thought of as one plane-wave field, which is known to produce no pairs. If the additional photon propagates into the opposite direction, then the pseudoenergy lines falls down such that it do not cross the kinetic energy lines, in contrast to the case in Fig. 5(a). This is because the photon momentum points into the direction in which the magnetic field accelerates the particles, leading to no intersection and hence infinite suppression of pair creation. As in the previous case, $|E| > |B|$, the direction of movement for the electron and positron along x is given by Eq. (26).

The imaginary part of the exponent for the electron now reads

$$W^- = i \frac{2}{3} \frac{[2e(Ep_{0,e} - Bp_{z,e})(x_s^- - x_e^-)]^{3/2}}{|2e(Ep_{0,e} - Bp_{z,e})|}. \quad (30)$$

For comparison, the same result will be derived in Appendix B by a different approach. Instead of the constant field approximation, the action integral W will be evaluated perturbatively in terms of the classical nonlinearity parameter $\xi = eE/(m\omega_L) \gg 1$ for the special case of an external plane-wave field with the characteristic frequency ω_L . For maximum

probability, the total exponent for pair production reduces to the value $4m^3/(3ek_0E)$. This is in accordance with the value already calculated in Ref. [49].

3.5. Case $|E| < |B|$

For this case, there is a minimal energy the quantized photon must have in order to produce a pair. Boosting into a reference frame, where the electric field vanishes, it is clear that no work will be done by the electromagnetic field. Hence, the whole energy in this frame for the pair must be carried by the quantized photon. In the case of no electric field and both the electron and positron carrying only their rest mass after creation, the quantized photon has to carry an energy of exactly $2m$, as shown in Fig. 5(c). Both kinetic energy lines are horizontal because of the electric field being zero, and their sum is equal to the initial photon energy of $2m$. If this initial energy would be smaller than $2m$, then the pseudoenergy lines would not hit the kinetic energy lines; instead, they would stay below them. This minimum energy condition is also given by Eq. (21), which yields for $E = 0$

$$k_0 = p_{0,e} + q_{0,e}. \quad (31)$$

The effect of a nonzero electric field may also be deduced from Fig. 5(c). A nonzero electric field tilts the kinetic energy lines to the one or the other direction, and consequently the exit points will be closer to or farther from x_s , and hence pair production will be enhanced or suppressed.

Interpreting Fig. 5(c) in terms of imaginary trajectories, it can be understood in the following way. At the point of pair production x_s , the momentum along the x direction for the electron and the positron has the value $\pm im$. The momentum along the z direction, transferred by the photon, is m . Following the imaginary trajectories from x_s on, the magnetic field rotates the momentum along the z direction onto the x direction and cancels exactly the initial imaginary momentum. Thus, the particles become real and pair production is possible. If the initial energy of the photon is smaller, then the magnetic field cannot turn the particles into real ones. If there is also an electric field, which reduces p_x and q_x in the same direction as the magnetic field, then the particles can leave the imaginary trajectory sooner, making pair production more probable. Pair production will be reduced or even completely cut off if the electric field works in the opposite direction, and therefore, the energy carried by the photon does not suffice anymore.

In contrast to the previous two cases, the direction of tunneling is now determined by the orientation of the B field and the quantized photon

$$\text{sgn } (x_e^+ - x_e^-) = -\text{sgn } (Bk_z). \quad (32)$$

If the electric field works in the tunneling direction, then the probability will be enhanced; otherwise it will be reduced. For $|E| < |B|$, the exponent for the electron computes to

$$W^- = i \frac{(Ep_{0,e} - Bp_{z,e})^2}{2\mathcal{E}^3} \left(\text{arcosh } \Gamma - \Gamma \sqrt{\Gamma^2 - 1} \right). \quad (33)$$

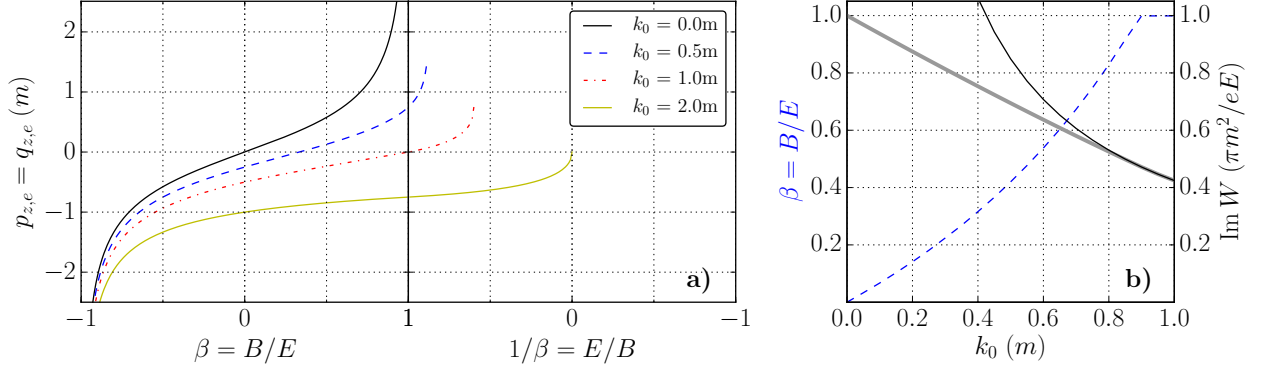


FIG. 6: (color online) Properties of the maximum probability trajectories. (a) The most probable z momentum at the tunneling exit of the electron and positron depending on the ratio $\beta = E/B$ and photon energy k_0 . The y momentum increases the relativistic mass of the particles and is therefore zero for maximum probability. By definition, the x momentum must be zero at the exit. For $\beta = 0$ (no magnetic field), the most probable z momentum is exactly half the photon momentum k_0 . Changing the magnetic field will introduce a shift of the momentum depending on the sign of β . In the right pane of part (a), where $|B| > |E|$, the lines end at some $0 < 1/\beta < 0$. This is due to the energy cutoff depending on the energy of the photon. (b) The optimum ratio β for a given photon energy k_0 to achieve maximal pair production probability. The dashed blue line gives the optimum ratio depending on k_0 , while the bold gray line gives its corresponding value for the exponent. At $k_0 = 0$, for example, it is best to have no magnetic field (Schwinger case). At $k_0 = k_0^* \equiv \sqrt{4/5} m$, the ratio β becomes 1, corresponding to the plane-wave case. The exponent for the plane-wave case is also given for reference by the thin black line. For $k_0 < k_0^*$, a tuned magnetic field can therefore enhance the pair production probability, while for values greater than $k_0 = k_0^*$, $\beta = 1$ is always optimal for a given fixed maximum field strength.

4. Maximum probability trajectories

Each tunneling trajectory is characterized by its final momenta of the created electron and positron and has a specific pair production probability, which depends on an exponential term with exponent $\text{Im } W = \text{Im } W^+ + \text{Im } W^-$ given in Eqs. (27), (30) and (33) as well as on a prefactor. The maximum probability trajectories are defined as the trajectories, where the exponential term $\text{Im } W$ is minimized for given electromagnetic field strengths E and B and a given photon energy k_0 . In general, the most probable trajectories are always the most symmetric ones. For the kinetic momenta at the exit, this means

$$p_{x,e} = q_{x,e} = 0, \quad (34a)$$

$$p_{y,e} = q_{y,e} = 0, \quad (34b)$$

$$p_{z,e} = q_{z,e}, \quad (34c)$$

where (34a) follows from the definition of the exit point and (34b) is required by minimizing the kinetic energy of the created particles.

The kinetic momenta $p_{z,e}$ and $q_{z,e}$ depend on the ratio $\beta = B/E$ as well on the momentum of the photon k_0 . Figure 6(a) illustrates the β -dependence of $p_{z,e}$ and $q_{z,e}$ for various k_0 . In the left part of Fig. 6(a) $|E| > |B|$, while in the right part $|E| < |B|$. At the center and at the outer borders, E and B have the same magnitude. For the Schwinger case with $B = 0$ and $k_0 = 0$, the final momentum of the maximum probability trajectories is zero, as shown in the figure. Varying β while keeping $k_0 = 0$ yields nonzero momenta $p_{z,e}$ and $q_{z,e}$, see solid black line in Fig. 6(a). The momentum $p_{z,e}$ corresponds exactly to the β boosted momentum of the zero momentum of $B = 0$. In the limit $|\beta| \rightarrow 1$, the momenta $p_{z,e}$ and $q_{z,e}$ and consequently the relativistic masses of the created particles diverge, which

is related to the fact that pair production is not allowed in this regime without a photon.

In the presence of a photon with momentum, the created electron and positron share the photon's momentum at x_s if $\beta = 0$ and keep it until the exit, because there is no magnetic field, and therefore, $p_{z,e} = q_{z,e} = k_0/2$ as also shown in Fig. 6(a). Going to the left of $\beta = 0$ shows that $p_{z,e}$ and $q_{z,e}$ diverge also for $k_0 > 0$, because the electric and the magnetic fields work into different directions. Going to the right of $\beta = 0$, they will work into the same region, and now pair production is also possible in the region $|\beta| > 1$, i. e., where $|B| > |E|$. For $k_0 < 2m$, the lines for the momenta $p_{z,e}$ and $q_{z,e}$ end before $1/\beta = 0$ because the photon's energy is not enough to create pairs without an electric field. The line for $k_0 = 2m$ ends exactly at $1/\beta = 0$ with $p_{z,e} = 0$. This corresponds to the case discussed in Fig. 5(c). Going further to the right of $1/\beta = 0$, the electric and magnetic field will work into opposite directions, and in this way render pair production impossible.

For a given photon momentum k_0 , pair creation may be maximized by varying β and minimizing the imaginary part of the exponent for the maximum probable trajectories. The corresponding exponent is shown in Fig. 6(b). The blue dashed line indicates the optimal ratio β . At $k_0 = 0$, it is optimal to have only an electric field. For $k_0 > 0$ also, the optimal β is nonzero, meaning that a magnetic field will enhance pair production. If the photon momentum is larger than the critical momentum

$$k_0^* \equiv \sqrt{4/5} m \approx 0.89 m \quad (35)$$

then the optimal β is 1, which corresponds to a plane wave. This means that, for a fixed maximum field strength, the plane-wave field is always optimum for photon energies larger than k_0^* , in the setup treated in this work. The value (35) may be

calculated by taking the derivative of Eq. (27) with respect to the magnetic field. This derivative is evaluated for the limit $B \rightarrow E$ and then set to zero, which gives an implicit equation for k_0^* that can be solved analytically. Note that k_0^* does not depend on the electromagnetic field magnitude E . The imaginary values of the exponent W are also shown in Fig. 6(b) for the plane-wave case (black solid line) and for the optimal case (gray solid line). The exponent for the optimum tuned case starts at $k_0 = 0$ with $i\pi m^2/(eE)$ (Schwinger case) and then decreases with increasing k_0 until it coincides with the value of the exponent for the plane-wave case at $k_0 = k_0^*$.

5. Conclusion

We introduced an intuitive tunneling picture for pair creation, which also incorporates effects due to a magnetic field and an additional high-energy photon. This picture is Lorentz invariant and does not depend on a particular gauge and is valid for homogeneous constant electromagnetic fields. This constant field approximation is valid, e. g., for the long wave limit of pair creation in counterpropagating laser fields.

The relativistic tunneling picture can be drawn due to the quasi-one-dimensional nature of the used setup in the quasistatic limit. Various features of pair creation can be inferred qualitatively from the introduced tunneling picture. For example, an additional photon lowers the potential barrier due to the photon's energy but also increases the particle's relativistic mass due to the photon's additional momentum. Due to this increased relativistic mass, the electron and positron stay longer (in terms of imaginary time) under the barrier until they gain enough energy to become real. An additional magnetic field, however, will also change the momentum under the barrier, and in this way, the relativistic mass. Depending on the magnetic field's direction and magnitude it may counteract the increase of the relativistic mass due to the photon's momentum and, therefore, increase the pair production probability.

The relativistic tunneling picture has been devised on the basis of a semiclassical approximation using classical trajectories. This approach also allowed us to calculate the exponents of the transition amplitudes. The calculated exponents for maximum probability agree with the analytical results by Nikishov [48] in the case of no incoming photon for the three different possibilities: $|E| > |B|$, $|E| = |B|$, and $|E| < |B|$. Furthermore, they agree with the results by Reiss [49], assuming a plane-wave external laser field with an incoming photon in the limit $\xi \ll 1$.

Other geometries, as well as time and space varying fields, may also be treated in the tunneling regime by imaginary trajectories, but their respective picture will be inherently multidimensional and hard to visualize. Nevertheless, simple trends due to time and space variation may be interpreted with the current picture, which will be subject to future work.

Acknowledgments

We are grateful to K. Z. Hatsagortsyan, A. Di Piazza, S. Meuren, and E. Yakoboylu for valuable discussions.

A. From quantum field theory to classical actions

This paragraph recapitulates how to derive the semiclassical approximation for matrix elements, which is usually symbolically written as

$$M_{fi} \sim \exp(-\text{Im } S). \quad (\text{A1})$$

This form in general is quite ambiguous, because the definition of the action S itself due to its gauge dependence is not unique, and furthermore it also depends on the type of initial and final states, which can be eigenstates of position, momentum or of a specific Hamiltonian (to name the most common).

Following the treatment in Ref. [45], the mode Hamiltonian \mathcal{H}_e of the matter part (e. g., electrons and positrons), describing the free modes of these particles is given by

$$\mathcal{H}_e = \alpha(-i\nabla) + \beta m. \quad (\text{A2})$$

The quantization leads to the following field Hamiltonian for the free quantized matter field:

$$\begin{aligned} \hat{H}_e &= \int d\mathbf{x} \hat{\psi}^\dagger(\mathbf{x}) \mathcal{H}_e \hat{\psi}(\mathbf{x}) \\ &= \int d\mathbf{x} \hat{\bar{\psi}}(\mathbf{x}) (-i\gamma\nabla + m) \hat{\psi}(\mathbf{x}). \end{aligned} \quad (\text{A3})$$

The same procedure applied to the free quantized radiation field leads to its corresponding field Hamiltonian \hat{H}_γ , which explicit form is not of interest here. The interaction between both fields is given by

$$\hat{H}_{\text{int,full}} = e \int d\mathbf{x} \hat{\bar{\psi}}(\mathbf{x}) \gamma_\mu \hat{\psi}(\mathbf{x}) \hat{A}_{\text{full}}^\mu(\mathbf{x}). \quad (\text{A4})$$

Both $\hat{\psi}(\mathbf{x})$ and $\hat{A}_{\text{full}}^\mu(\mathbf{x})$ are the field operators of the quantized matter and radiation field in the Schrödinger picture, whence they only depend on \mathbf{x} . This theory describes the full QED. But, so far, it does not allow to solve even very simple problems, and hence some approximations need to be done. The most fundamental approximation, as is common for problems of QED in external fields, is the separation of the full electromagnetic field into a quantized radiation field $\hat{A}^\mu(\mathbf{x})$ and a classical external field $A_{\text{ext}}^\mu(\mathbf{x})$. Treating the external field as a classical field is motivated by the fact that it should be very intense and quantum effects are negligible. Its interaction with the matter field is given by the following Hamiltonian:

$$\hat{H}_{\text{int,ext}} = e \int d\mathbf{x} \hat{\bar{\psi}}(\mathbf{x}) \gamma_\mu \hat{\psi}(\mathbf{x}) A_{\text{ext}}^\mu(\mathbf{x}). \quad (\text{A5})$$

Note the explicit time dependence of this Hamiltonian due to the possible time dependence of $A_{\text{ext}}^\mu(x)$. A further important fact of the external field approximation is neglecting the influence of the matter field on the dynamics of the external field, also called backreaction. That way, $A_{\text{ext}}^\mu(x)$ is assumed to behave like a classical free electromagnetic field that does not see the current

$$\hat{j}^\mu = e \hat{\bar{\psi}} \gamma_\mu \hat{\psi} \quad (\text{A6})$$

created by the matter field. Putting together \hat{H}_e and $\hat{H}_{\text{int,ext}}$ gives the (possible time-dependent) quantized field Hamiltonian for the matter field in an external field,

$$\begin{aligned} \hat{H}_{e,\text{ext}} &= \hat{H}_e + \hat{H}_{\text{int,ext}} \\ &= \int d\mathbf{x} \hat{\bar{\psi}}(\mathbf{x}) \left[\gamma(-i\nabla - \mathbf{A}_{\text{ext}}) + m + e\gamma^0 A_{\text{ext}}^0 \right] \hat{\psi}(\mathbf{x}). \end{aligned} \quad (\text{A7})$$

Thus, the modes of the matter field in the external electromagnetic field are described by the following Hamiltonian, known as the Dirac Hamiltonian with an external field:

$$\mathcal{H}_{e,\text{ext}} = \alpha(-i\nabla - \mathbf{A}_{\text{ext}}) + \beta m + eA_{\text{ext}}^0, \quad (\text{A8})$$

and therefore they take the influence of the external field into full account. The interaction with the quantized field is still treated perturbatively. For doing this, it is convenient to switch to the interaction picture, with the free part

$$\hat{H}_0 = \hat{H}_\gamma + \hat{H}_{e,\text{ext}} \quad (\text{A9})$$

and the interaction part

$$\hat{H}_{\text{int}} = e \int d\mathbf{x} \hat{\bar{\psi}}(\mathbf{x}) \gamma_\mu \hat{\psi}(\mathbf{x}) \hat{A}^\mu(\mathbf{x}). \quad (\text{A10})$$

This type of interaction picture, including the interaction with the external field in \hat{H}_0 , is also called the Furry picture [46]. The field operator for the matter field becomes time dependent (\hat{U}_0 being the unitary operator, transforming from the Schrödinger to the interaction picture),

$$\hat{\psi}_I(x) = \hat{U}_0^\dagger \hat{\psi}(x) \hat{U}_0, \quad (\text{A11})$$

and it can be shown that this field operator will solve the Dirac equation in the external field

$$(i\partial_t - \mathcal{H}_{e,\text{ext}}) \hat{\psi}_I(x) = 0. \quad (\text{A12})$$

Knowing this, the field operator $\hat{\psi}_I$ can be expanded into a complete set of eigensolutions (modes). There are, of course, infinitely many different sets. The two sets $\pm\varphi_n(x)$ and $\pm\varphi_n(x)$ are chosen, satisfying the relations

$$\mathcal{H}_{e,\text{ext}}(t_{\text{in}}) \pm\varphi_n(\mathbf{x}t_{\text{in}}) = \pm\varepsilon_n \pm\varphi_n(\mathbf{x}t_{\text{in}}), \quad (\text{A13a})$$

$$\mathcal{H}_{e,\text{ext}}(t_{\text{out}}) \pm\varphi_n(\mathbf{x}t_{\text{out}}) = \pm\varepsilon_n \pm\varphi_n(\mathbf{x}t_{\text{out}}). \quad (\text{A13b})$$

Thus, the set $\pm\varphi_n(x)$ corresponds to positive/negative-energy eigensolutions ($\pm\varepsilon_n \geq 0$) at t_{in} , and $\pm\varphi_n$ to positive/negative-energy eigensolutions ($\pm\varepsilon_n \geq 0$) at t_{out} . Using these sets, the field operator can be expanded as

$$\hat{\psi}_I(x) = \sum_n \hat{a}_n(\text{in}) \varphi_n(x) + \hat{b}_n^\dagger(\text{in}) \bar{\varphi}_n(x) \quad (\text{A14a})$$

$$= \sum_n \hat{a}_n(\text{out}) \varphi_n(x) + \hat{b}_n^\dagger(\text{out}) \bar{\varphi}_n(x), \quad (\text{A14b})$$

defining also two possible different sets of creation/annihilation operators, \hat{a}^\pm/\hat{a} and \hat{b}^\pm/\hat{b} , for positive and negative energy particles at t_{in} and t_{out} . These in turn define the vacuum states at t_{in} and t_{out} :

$$\hat{a}_n(\text{in})|0, \text{in}\rangle = 0, \quad \hat{b}_n(\text{in})|0, \text{in}\rangle = 0, \quad (\text{A15a})$$

$$\hat{a}_n(\text{out})|0, \text{out}\rangle = 0, \quad \hat{b}_n(\text{out})|0, \text{out}\rangle = 0. \quad (\text{A15b})$$

1. Pair production due to the external electromagnetic field only

By considering the external electromagnetic field only (zeroth order in the quantized radiation field), the time evolution operator in the interaction picture ($\hat{H}_{\text{int,I}}$ being the interaction picture representation of Eq. (A10)) reduces to the identity, that is,

$$\begin{aligned} \hat{U}(t_{\text{out}}, t_{\text{in}}) &= \mathcal{T} \exp \left[-i \int_{t_{\text{in}}}^{t_{\text{out}}} \hat{H}_{\text{int,I}} dt \right] \\ &\rightarrow \hat{1} \quad (\text{in 0th order}). \end{aligned} \quad (\text{A16})$$

Thus, as shown in Ref. [45], for all the transition elements of interest, one only needs to know the following propagator elements:

$$G(\zeta|_{\kappa})_{mn} = \int d\mathbf{x} d\mathbf{y} \zeta \varphi_m^+(\mathbf{x}t_{\text{out}}) G(\mathbf{x}t_{\text{out}}, \mathbf{y}t_{\text{in}}) \varphi_n(\mathbf{y}t_{\text{in}}), \quad (\text{A17})$$

$$G(\kappa|_{\kappa}) = G(\zeta|_{\kappa})^+, \quad (\text{A18})$$

with m, n being the quantum numbers of the modes at $t_{\text{out/in}}$ and $\zeta, \kappa = \pm$ denoting positive or negative energy (i. e., particle or antiparticle). $G(\mathbf{x}t_{\text{out}}, \mathbf{y}t_{\text{in}})$ is the full propagator of Eq. (A8). These propagator elements represent the probability that a positive/negative mode from t_{in} evolves into a positive/negative mode at t_{out} . According Ref. [45], the vacuum stability up to zeroth order in the quantized radiation field is given by the transition amplitude between $|0, \text{in}\rangle$ and $|0, \text{out}\rangle$:

$$c_v = \langle 0, \text{out} | 0, \text{in} \rangle = \det G^+(\cdot|_{+}) = \det G^-(\cdot|_{-}). \quad (\text{A19})$$

Furthermore, the transition amplitude for producing one pair that is evolving from an initial vacuum state $|0, \text{in}\rangle$ to a pair state $|n, m, \text{out}\rangle$ (electron/positron having quantum number n/m) yields

$$\begin{aligned} \langle n, m, \text{out} | 0, \text{in} \rangle &= \langle 0, \text{out} | a_m(\text{out}) b_n(\text{out}) | 0, \text{in} \rangle \\ &\equiv \omega(\bar{m}\bar{n})|0\rangle c_v, \end{aligned} \quad (\text{A20})$$

with

$$\omega(\bar{m}\bar{n})|0\rangle = \left[G^{-1}(\cdot|_{+}) G(\cdot|_{-}) \right]_{mn} = - \left[G(\cdot|_{-}) G^{-1}(\cdot|_{-}) \right]_{mn}. \quad (\text{A21})$$

For the semiclassical case, where pair production is exponentially suppressed, it is possible to write

$$c_v = 1 + \mathcal{O}(e^-), \quad (\text{A22a})$$

$$G(\cdot|_{+})_{mn} = e^{i\theta_n^+} \delta_{mn} + \mathcal{O}(e^-), \quad (\text{A22b})$$

$$G(\cdot|_{-})_{mn} = e^{i\theta_n^-} \delta_{mn} + \mathcal{O}(e^-), \quad (\text{A22c})$$

$$G(\cdot|_{+})_{mn} = \mathcal{O}(e^-), \quad (\text{A22d})$$

$$G(\cdot|_{-})_{mn} = \mathcal{O}(e^-). \quad (\text{A22e})$$

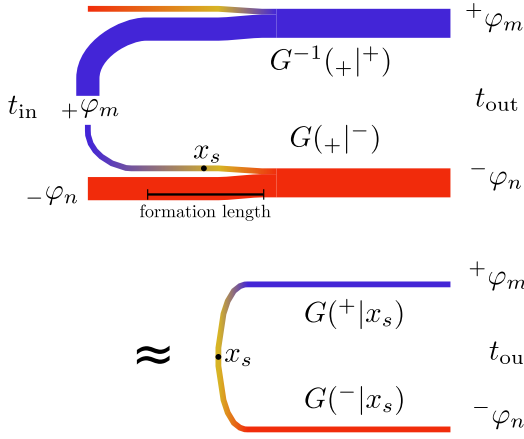


FIG. 7: Visualization of the single pair production element of Eq. (A21). Both positive and negative modes (bold) propagate back in time. Only an exponentially suppressed part (thin) splits up and evolves into different modes. The different modes under consideration must match at t_{in} . In the semiclassical approximation, the transition element can be approximated by the classical trajectory, that connects both the electron and positron at t_{out} with their initial point of creation x_s . The formation length gives the typical timescale that is needed for splitting up a different mode from the main mode

The notation $\mathcal{O}(e^-)$ stands for the exponentially small corrections. Physically, this means that the positive/negative modes at t_{in} mainly evolve into their corresponding positive/negative modes at t_{out} up to a phase θ^+/θ^- . Only an exponentially small fraction of their norm goes into different modes, regardless of whether they are positive or negative. Inverting $G(+|_+)$ and $G(-|_-)$ yields, therefore,

$$G(+|_+)^{-1}_{mn} = e^{-i\theta^+_{mn}} \delta_{mn} + \mathcal{O}(e^-), \quad (\text{A23})$$

$$G(-|_-)^{-1}_{mn} = e^{-i\theta^-_{mn}} \delta_{mn} + \mathcal{O}(e^-). \quad (\text{A24})$$

Plugging this into the first line of Eq. (A21) results in

$$\omega(mn|0) = e^{i\theta^+_{mn}} G(+|_-)_{mn} + \mathcal{O}^2(e^-). \quad (\text{A25})$$

Thus, up to first order in the exponential suppression, the single pair production elements in Eq. (A21) are given by the matrix $G(+|_-)$ or alternatively by $G(+|_-)$. The matrix element $G(+|_-)_{mn}$ gives the overlap between the negative mode $-\varphi_n$, propagated from t_{out} to t_{in} , with the positive mode $+\varphi_m$ at t_{in} . Explicitly, this reads

$$G(+|_-)_{mn} = \int d\mathbf{x}' d\mathbf{x} \varphi_m^+(\mathbf{x}') G(\mathbf{x}' t_{\text{in}}, \mathbf{x} t_{\text{out}}) \varphi_n^-(\mathbf{x}). \quad (\text{A26})$$

This means that somewhere in between t_{out} and t_{in} , a small part of $-\varphi_n$ splits up and evolves into $+\varphi_m$. Still, the main part goes into $-\varphi_n$ ($G(-|_-)$). This is shown schematically in the upper part of Fig. 7. Also shown there is a length, the so-called formation length, because typically the timescale on which the conversion from $-\varphi_n$ to $+\varphi_m$ happens is finite. By finite, we mean that only exponentially small corrections occur if the formation length is increased further. In this sense, the formation length is not strictly defined; rather, it gives some

estimate for the timescale on which most of the conversion has already happened (see also Ref. [50] for the case of a constant electromagnetic field).

The real space propagator is approximated in the semiclassical approximation by

$$G(\mathbf{x}' t', \mathbf{x} t) \sim \exp[iS(\mathbf{x}' t', \mathbf{x} t)]. \quad (\text{A27})$$

Similarly, the propagator from a momentum eigenstate to another (in our notation taking the quantum numbers $n = \mathbf{p}$ and $m = \mathbf{q}$) is approximated semiclassically as

$$G(\mathbf{p} t', \mathbf{q} t) \sim \exp[iS(\mathbf{x}' t', \mathbf{x} t) - i\mathbf{P}\mathbf{x}' + i\mathbf{Q}\mathbf{x}] \quad (\text{A28})$$

with \mathbf{x}' and \mathbf{x} implicitly given by

$$\mathbf{P} = \left. \frac{\partial S}{\partial \mathbf{x}'} \right|_{\mathbf{x}'} \quad \text{and} \quad \mathbf{Q} = \left. \frac{\partial S}{\partial \mathbf{x}} \right|_{\mathbf{x}}. \quad (\text{A29})$$

The additional terms are due to the in- and out-modes being momentum and not position eigenstates, see also Refs. [51, 52]. Thus, the full propagator gets approximated only by its classical trajectory connecting the appropriate in- and out-modes instead of all trajectories in the path integral picture. One peculiarity of Eq. (A28) is the matrix structure of its left-hand side corresponding to the full propagator. Its right-hand side does not have this matrix structure, as the exponential is a scalar. As shown in Ref. [53], the semiclassical treatment of the Dirac equation leads to a prefactor with matrix structure, which must not be necessarily diagonal in the zeroth order of \hbar . Therefore, a transition from a positive-energy spinor to a negative-energy spinor is possible. Nevertheless, the main contribution to the matrix elements stems from the exponential factor. In the classical picture, the transition from a negative-energy eigenstate to a positive must happen on an imaginary trajectory, because an electron with positive energy will always stay an electron with positive energy on a real trajectory. But if it goes over to an imaginary path and wraps around the root of its kinetic energy $p_0 = \sqrt{m^2 + \mathbf{p}^2}$, it is possible that it continues on the other branch of the square root—that is, $p_0 = -\sqrt{m^2 + \mathbf{p}^2}$ —and therefore becomes a negative energy electron. This point on the imaginary part of the trajectory, where this transition occurs, might be defined by $p_0 = 0$ and will be denoted by x_s . It should be mentioned that it has no direct physical meaning; i. e., it cannot be measured. Nevertheless, it can be related to the region of the formation length. Using this point as the point of pair production in the classical picture, the propagator in Eq. (A28) can be split into

$$G(\mathbf{p} t_{\text{in}}, \mathbf{q} t_{\text{out}}) \sim e^{iS(\mathbf{x}' t_{\text{in}}, x_s) - i\mathbf{P}\cdot\mathbf{x}'} e^{iS(x_s, \mathbf{x} t_{\text{out}}) + i\mathbf{Q}\cdot\mathbf{x}}, \quad (\text{A30})$$

where the back part corresponds to a negative energy electron traveling back in time from t_{out} to $x_{0,s}$, which can also be interpreted as a positron going from $x_{0,s}$ to t_{out} (changing sign in \mathbf{q} and charge). For the full matrix element in Eq. (A21), the front part of Eq. (A30) gets multiplied by $G(+|_+)^{-1}$. In our approximation this corresponds to a propagation of the positive-energy electron back from t_{in} to t_{out} , and one can therefore write

$$G(+|_+)^{-1} e^{iS(\mathbf{x}' t_{\text{in}}, x_s) - i\mathbf{P}\cdot\mathbf{x}'} \sim e^{iS(\mathbf{x}' t_{\text{out}}, x_s) - i\mathbf{Q}\cdot\mathbf{x}'} \quad (\text{A31})$$

Accordingly, the transition element in Eq. (A21) can now be written as

$$\omega(m\bar{n}|0) = \exp[-\text{Im}(W_p + W_q)], \quad (\text{A32})$$

where $W_p = S(\mathbf{x}'t_{\text{out}}, x_s) - \mathbf{P} \cdot \mathbf{x}'$ and $W_q = S(\mathbf{x}t_{\text{out}}, x_s) - \mathbf{Q} \cdot \mathbf{x}$ correspond to the modified actions of the electron and positron along their classical imaginary trajectories. This result is schematically drawn in the lower part of Fig. 7 with $G^{(+)}|x_s) \sim e^{iW_p}$ and $G^{(-)}|x_s) \sim e^{iW_q}$. If there are, for a specific field configuration, different imaginary paths possible for connecting the electron and positron in their specific out-states, their contribution must be added and might lead to interference phenomena.

2. Pair production due to perturbative treatment of the quantized electromagnetic field

For this case, the first-order correction to the time evolution operator in Eq. (A16) is given by

$$\begin{aligned} \hat{U}(t_{\text{out}}, t_{\text{in}}) &\rightarrow -i \int_{t_{\text{in}}}^{t_{\text{out}}} \hat{H}_{\text{int}, I} dt \\ &\rightarrow -ie \int \hat{\psi}_I(x) \gamma^\mu \hat{\psi}_I(x) \hat{A}_I^\mu(x) dx. \end{aligned} \quad (\text{A33})$$

The field operators in their interaction representation can be expanded (as before) into the solutions of their corresponding mode Hamiltonians. For the matter field operator $\hat{\psi}_I$, the decomposition Eq. (A14b) for the out-states is used again, as the main interest lies in pair creation and not pair annihilation. The field operator for the free quantized electromagnetic field is decomposed as

$$\hat{A}^\mu(x) = \sum_{\lambda=0}^3 \int [\hat{c}_{k\lambda} f_{k\lambda}^\mu(x) + \hat{c}_{k\lambda}^+ f_{k\lambda}^{\mu*}(x)] d\mathbf{k}, \quad (\text{A34})$$

and $f_{k\lambda}^\mu(x)$ being the photon wave function proportional to [54]

$$f_{k\lambda}^\mu(x) \sim \exp[-ikx] = \exp[iW_k(x)], \quad (\text{A35})$$

where $W_k(x) = -kx$ usually is called its classical action. Care should be taken here, since this action does not correspond to an action of the type $S(\mathbf{x}', x)$ but rather to the modified action discussed before, where on one side the momentum k and on the other side the spacetime x is fixed.

Expressing also the solutions ${}^\pm\varphi_n$ to the Dirac equation in their semiclassical approximation and setting the final quantum number n to momentum eigenstates (p for the electron and q for the positron), they read ${}^+\varphi_n(x) \sim \exp[-iW_p(x)]$ and ${}^-\varphi_n(x) \sim \exp[+iW_q(x)]$ for the electron and the positron, respectively. The “+” in the positron’s exponent is due to its quantization as an antiparticle. Again, W_p and W_q are usually called the electron and positron classical actions, but the same distinction as mentioned before applies here. Note that in the case of an external plane-wave field, these actions are given by the

so-called Volkov actions, and the semiclassical exponent is exact.

By taking into account the first order of the interaction with the quantized field, pair production can now happen with the additional help of an incoming quantized photon. The in-state is defined as

$$|0, 0, 1_k\rangle \equiv \hat{c}_k^+ |0, \text{in}\rangle, \quad (\text{A36})$$

and the out-state as

$$|1_p, 1_q, 0\rangle \equiv \hat{a}_p^+(\text{out}) \hat{b}_q^+(\text{out}) |0, \text{out}\rangle. \quad (\text{A37})$$

The transition amplitude for this process to first order is given by

$$M_{fi} = -ie \langle 1_p, 1_q, 0 | \int \hat{\psi}_I(x) \gamma^\mu \hat{\psi}_I(x) \hat{A}_I^\mu(x) dx | 0, 0, 1_k \rangle. \quad (\text{A38})$$

Expanding the field operators according to Eqs. (A14b) and (A34) and writing (approximating) the field mode solutions in terms of their modified classical action W yields

$$M_{fi} \sim -ie c_v \int dx e^{[i(W_k(x) + W_p(x) + W_q(x))]}. \quad (\text{A39})$$

Applying the method of stationary phase to this integral yields the following condition for a stationary phase:

$$\begin{aligned} 0 &= \frac{\partial}{\partial x^\mu} (W_k + W_p + W_q)|_{x_s} \\ &= K^\mu(x_s) - P^\mu(x_s) - Q^\mu(x_s) \\ &= k^\mu(x_s) - p^\mu(x_s) - q^\mu(x_s). \end{aligned} \quad (\text{A40})$$

The last line follows from the previous one due to the fact that the gauges at the same spacetime point (x_s) cancel each other exactly [55]. Note that the modified actions W , which depend on momentum and space, are used in the derivation of Eq. (A40) and not the usual actions S , which depend on two positions. Although the modified actions W are gauge dependent, the point of stationary phase x_s is given by a gauge-independent and Lorentz-invariant kinetic equation, which can be interpreted from a classical point of view. According to Eq. (A39), the matrix element is an interference from all spacetime points x where the photon converts into electron and positron obeying the asymptotic momenta. The outcome of this interference, e. g., the matrix element, can be approximated by the point of stationary phase. Due to energy-momentum conservation $p + q = k$ at this point, the laws of classical mechanics are satisfied. Therefore, the particle conversion stemming from the creation and annihilation operators in quantum field theory can be brought to a classical level in the semiclassical approximation.

The classical trajectory will now look like an incoming photon that will convert at x_s instantaneously into an electron and positron while satisfying energy-momentum conservation. The electron and positron will travel further in the external field and approach their asymptotic momenta.

The condition $p + q = k$ cannot be satisfied in real spacetime, as can be seen by squaring both sides of this equation, but in imaginary spacetime. This leads to an imaginary classical trajectory. Therefore, approximating Eq. (A39) semiclassically yields

$$M_{fi} \sim -ie c_V e^{-\text{Im}(W_k + W_p + W_q)}. \quad (\text{A41})$$

B. Perturbative evaluation of the exponent for the plane-wave case

For the plane-wave four-potential, we choose the following gauge (with $\eta = k_L x$ being the phase of the laser, E the maximum field amplitude and $\omega_L = k_{L,0}$ the characteristic frequency):

$$A_\mu(\eta) = \left(0, \frac{E}{\omega_L} f(\eta), 0, 0\right), \quad (\text{B1})$$

yielding for the electron the constants of motion (according to Eq. (3)) $P_x, P_y = p_y$, and $P_0 - P_z = p_0 - p_z$. The last expression can be written in a Lorentz-invariant way, $\Lambda_p = k_L p$. Accordingly, the same is true for the positron. For the quantized photon, this notation can be used too, $\Lambda_k = k_L k$, yielding also a constant of motion.

To make use of these constants of motion, the transformation

$$(t, x, y, z) \rightarrow (\eta, x', y', z') = (k_L(t - z), x, y, z/k_L) \quad (\text{B2})$$

into a different coordinate system is applied (x, y and z are spacetime coordinates and not four-vectors in this paragraph). The total differential of the spacetime-dependent part of the action W in this coordinate system

$$W(x, y, z, t) = W(x', y', z', t(z', \eta)) \quad (\text{B3})$$

is given for the electron and analogously for the positron by

$$dW(x', y', z', \eta) = -P_x dx' - P_y dy' + \omega_L(P_0 - P_z) dz' + P_0/\omega_L d\eta, \quad (\text{B4})$$

which can be written in the gauge of Eq. (B1) as

$$dW(x', y', z', \eta) = -P_x dx' - P_y dy' + \Lambda_p dz' + \frac{p_0}{\omega_L} d\eta. \quad (\text{B5})$$

The first three terms are the constants of motion and can be integrated:

$$W(x', y', z', \eta) = -P_x x' - P_y y' + \Lambda_p z' + \int^\eta \frac{p_0}{\omega_L} d\varphi. \quad (\text{B6})$$

Similarly, the photon's action can be written this way:

$$W(x', y', z', \eta) = k_x x' + k_y y' - \Lambda_k z' - \int^\eta \frac{k_0}{\omega_L} d\varphi. \quad (\text{B7})$$

Allowing only for the classical trajectory—that is, four-momentum conservation at the point of pair creation—yields the following set of constraints:

$$P_x + Q_x = p_x + q_x = 0, \quad (\text{B8a})$$

$$P_y + Q_y = p_y + q_y = 0, \quad (\text{B8b})$$

$$\Lambda_p + \Lambda_q = \Lambda_k, \quad (\text{B8c})$$

$$p_0(\eta_s) + q_0(\eta_s) = k_0. \quad (\text{B8d})$$

The last line, Eq. (B8d), implicitly determines the phase η_s of the electromagnetic field, where the pair will be produced on the classical trajectory. This trajectory, as well as η_s , has to be imaginary. Again, this imaginary trajectory will not be the physical trajectory of the process. It is only the trajectory where the exponential part of the matrix element gets stationary and hence yields a good approximation for its value. The part of the exponent which has an imaginary value is given by the sum of the actions of the electron, positron and photon:

$$\Sigma W = \frac{1}{\omega_L} \left(\int^{\eta_s} p_0 d\varphi + \int^{\eta_s} q_0 d\varphi - \int^{\eta_s} k_0 d\varphi \right). \quad (\text{B9})$$

In the general case, η_s and subsequently $\text{Im} \Sigma W$ need to be calculated depending on the analytic form of the given electromagnetic field. Usually, this has to be done numerically. In the case of the classical nonlinearity parameter $\xi = eE_0/m\omega_L$ being much larger than 1, the integral can be calculated perturbatively up to order $\mathcal{O}(1/\xi)$ and gives the same results as a constant crossed field with $|E| = |B|$ as shown in the following. Using the identity

$$\Lambda_p = k_L p = \omega_L (p_0 - p_z) \quad (\text{B10})$$

it follows

$$p_z = p_0 - \frac{\Lambda_p}{\omega_L}, \quad (\text{B11})$$

$$p_z^2 = m^2 + p_x^2 + p_y^2 + p_z^2 - 2p_0 \frac{\Lambda_p}{\omega_L} + \frac{\Lambda_p^2}{\omega_L^2}, \quad (\text{B12})$$

$$p_0 = \frac{\omega_L}{2\Lambda_p} (m^2 + p_x^2 + p_y^2) + \frac{\Lambda_p}{2\omega_L}, \quad (\text{B13})$$

and from Eqs. (B8) and (4),

$$p_x(\eta) = -q_x(\eta) \rightarrow p_x^2(\eta) = q_x^2(\eta). \quad (\text{B14})$$

Plugging Eqs. (B13) and (B14) into Eq. (B9) and using Eq. (B8c) gives

$$\Sigma W = -\left(\frac{1}{2\Lambda_p} + \frac{1}{2\Lambda_q} \right) \int^{\eta_s} d\varphi [m_*^2 + p_x^2(\varphi)]. \quad (\text{B15})$$

η_s is implicitly fixed by Eq. (B8d), leading to

$$p_x(\eta_s) = \pm im_*, \quad (\text{B16})$$

with m_* being defined as in Eq. (12). Using the four-potential Eq. (B1) and rewriting in terms of the canonical momentum P_x (constant of motion) yields

$$\pm i \frac{1}{\xi} + \frac{\omega_L P_x}{eE_0} = f(\eta_s) \quad \text{with} \quad \xi = \frac{eE_0}{m_* \omega_L}. \quad (\text{B17})$$

Assuming ξ being large, η_s can be evaluated perturbatively in powers of $1/\xi$ as

$$\eta_s = \eta_s^0 + \frac{1}{\xi}\eta_s^1 + \frac{1}{\xi^2}\eta_s^2 + \dots \quad (\text{B18})$$

Solving Eq. (B17) up to first order in $1/\xi$ gives

$$\eta_s^0 = f^{-1}\left(\frac{\omega_L P_x}{eE_0}\right), \quad (\text{B19})$$

$$\eta_s^1 = \pm i/f'(\eta_s^0). \quad (\text{B20})$$

Only the part $\eta_s^0 \rightarrow \eta_s^0 + \eta_s^1/\xi$ of the integration contour for ΣW gives an imaginary contribution (in $O(1/\xi)$), and therefore the integral needs to be calculated just along this path. The integrand of ΣW is rewritten as

$$m_*^2 + p_x^2 = m_*^2 \left(1 + \frac{p_x^2}{m_*^2}\right) = m_*^2 \left[1 + \left(\frac{P_x}{m_*} - \xi f(\varphi)\right)^2\right], \quad (\text{B21})$$

and expanding $f(\varphi)$ around η_s^0 ,

$$f(\varphi) \sim f(\eta_s^0) + f'(\eta_s^0)(\varphi - \eta_s^0) + \dots, \quad (\text{B22})$$

yields

$$m_*^2 + p_x^2 \sim m_*^2 \left[1 + \left[\xi f'(\eta_s^0)(\varphi - \eta_s^0)\right]^2\right]. \quad (\text{B23})$$

Consequently, ΣW calculates to

$$\begin{aligned} &\sim m_*^2 \int_{\eta_s^0}^{\eta_s^0 + \eta_s^1/\xi} d\varphi \left[1 + \left[\xi f'(\eta_s^0)(\varphi - \eta_s^0)\right]^2\right] \\ &= \pm i \frac{2}{3} \frac{m_*^2}{\xi f'(\eta_s^0)} + O\left(\frac{1}{\xi^2}\right). \end{aligned} \quad (\text{B24})$$

Taking the correct sign of $\pm i$ for exponential suppression and writing ξ explicitly gives the final result

$$\Sigma W = W^- + W^+ = \frac{i}{3} \frac{m_*^3}{\Lambda_p} \frac{\omega_L}{eE(\eta_s^0)} + \frac{i}{3} \frac{m_*^3}{\Lambda_q} \frac{\omega_L}{eE(\eta_s^0)}. \quad (\text{B25})$$

Taking only the electron part W^- and rewriting it as

$$W^- = \frac{i}{3} \frac{m_*^3}{\omega_L(p_0 - p_z)} \frac{\omega_L}{eE(\eta_s^0)} = \frac{i}{3} \frac{m_*^3}{p_0 - p_z} \frac{1}{eE(\eta_s^0)}, \quad (\text{B26})$$

it can be seen that this yields the same result as the constant field approximation in Eq. (30) by using the identities $B = -Ek_z/k_0$ and $p_{0,e}^2 - p_{z,e}^2 = m_*^2$. This is because the expansion only up to the order $O(1/\xi)$ corresponds to expanding the external field up to its first derivative, giving a constant crossed field.

-
- [1] F. Sauter, *Z. Phys.* **69**, 742 (1931).
 - [2] W. Heisenberg and H. Euler, *Z. Phys.* **98**, 714 (1936).
 - [3] J. Schwinger, *Phys. Rev.* **82**, 664 (1951).
 - [4] E. Brezin and C. Itzykson, *Phys. Rev. D* **2**, 1191 (1970).
 - [5] F. Ehlotzky, K. Krajewska, and J. Z. Kamiński, *Rep. Prog. in Phys.* **72**, 046401 (2009).
 - [6] R. Ruffini, G. Vereshchagin, and S.-S. Xue, *Phys. Rep.* **487**, 1 (2010).
 - [7] A. Di Piazza, C. Müller, K. Z. Hatsagortsyan, and C. H. Keitel, *Rev. Mod. Phys.* **84**, 1177 (2012).
 - [8] H. Gies and K. Klingmüller, *Phys. Rev. D* **72**, 065001 (2005).
 - [9] M. Ruf, G. R. Mocken, C. Müller, K. Z. Hatsagortsyan, and C. H. Keitel, *Phys. Rev. Lett.* **102**, 080402 (2009).
 - [10] G. R. Mocken, M. Ruf, C. Müller, and C. H. Keitel, *Phys. Rev. A* **81**, 022122 (2010).
 - [11] F. Hebenstreit, R. Alkofer, and H. Gies, *Phys. Rev. Lett.* **107**, 180403 (2011).
 - [12] I. V. Sokolov, N. M. Naumova, J. A. Nees, and G. A. Mourou, *Phys. Rev. Lett.* **105**, 195005 (2010).
 - [13] T.-O. Müller and C. Müller, *Phys. Rev. A* **86**, 022109 (2012).
 - [14] S. Augustin and C. Müller, *Phys. Rev. A* **88**, 022109 (2013).
 - [15] K. Krajewska, C. Müller, and J. Z. Kamiński, *Phys. Rev. A* **87**, 062107 (2013).
 - [16] R. Schützhold, H. Gies, and G. Dunne, *Phys. Rev. Lett.* **101**, 130404 (2008).
 - [17] G. V. Dunne, H. Gies, and R. Schützhold, *Phys. Rev. D* **80**, 111301 (2009).
 - [18] A. Di Piazza, E. Lötstedt, A. I. Milstein, and C. H. Keitel, *Phys. Rev. Lett.* **103**, 170403 (2009).
 - [19] B. King, H. Gies, and A. Di Piazza, *Phys. Rev. D* **86**, 125007 (2012).
 - [20] K. Krajewska and J. Z. Kamiński, *Phys. Rev. A* **86**, 052104 (2012).
 - [21] S. P. Kim and D. N. Page, *Phys. Rev. D* **73**, 065020 (2006).
 - [22] Q. Su, W. Su, Q. Z. Lv, M. Jiang, X. Lu, Z. M. Sheng, and R. Grobe, *Phys. Rev. Lett.* **109**, 253202 (2012).
 - [23] W. Su, M. Jiang, Z. Q. Lv, Y. J. Li, Z. M. Sheng, R. Grobe, and Q. Su, *Phys. Rev. A* **86**, 013422 (2012).
 - [24] Q. Z. Lv, Y. J. Li, R. Grobe, and Q. Su, *Phys. Rev. A* **88**, 033403 (2013).
 - [25] F. Hebenstreit, J. Berges, and D. Gelfand, *Phys. Rev. D* **87**, 105006 (2013).
 - [26] Y. Liu, M. Jiang, Q. Z. Lv, Y. T. Li, R. Grobe, and Q. Su, *Phys. Rev. A* **89**, 012127 (2014).
 - [27] F. Hebenstreit and J. Berges, *Phys. Rev. D* **90**, 045034 (2014).
 - [28] M. Jiang, Q. Z. Lv, Y. Liu, R. Grobe, and Q. Su, *Phys. Rev. A* **90**, 032101 (2014).
 - [29] K. Kohlfirst, H. Gies, and R. Alkofer, *Phys. Rev. Lett.* **112**, 050402 (2014).
 - [30] G. A. Mourou, T. Tajima, and S. V. Bulanov, *Rev. Mod. Phys.* **78**, 309 (2006).
 - [31] G. A. Mourou, N. J. Fisch, V. M. Malkin, Z. Toroker, E. A. Khazanov, A. M. Sergeev, T. Tajima, and B. Le Garrec, *Opt. Commun.* **285**, 720 (2012).
 - [32] N. Szpak and R. Schützhold, *New J. Phys.* **14**, 035001 (2012).
 - [33] A. M. Fedotov, N. B. Narozhny, G. Mourou, and G. Korn, *Phys.*

- Rev. Lett. **105**, 080402 (2010).
- [34] V. S. Popov, Sov. Phys. JETP **34**, 709 (1972).
 - [35] L. V. Keldysh, Sov. Phys. JETP **20**, 1307 (1965).
 - [36] V. S. Popov, Sov. Phys. JETP **36**, 840 (1973).
 - [37] V. S. Popov, Phys. Atom. Nucl. **68**, 686 (2005).
 - [38] S. V. Popruzhenko, V. D. Mur, V. S. Popov, and D. Bauer, Phys. Rev. Lett. **101**, 193003 (2008).
 - [39] S. Popruzhenko, V. Mur, V. Popov, and D. Bauer, Sov. Phys. JETP **108**, 947 (2009).
 - [40] H. M. Castañeda Cortés, S. V. Popruzhenko, D. Bauer, and A. Pálffy, New J. Phys. **13**, 063007 (2011).
 - [41] H. R. Reiss, Phys. Rev. Lett. **101**, 043002 (2008).
 - [42] H. R. Reiss, J. Phys. B: At., Mol. Opt. Phys. **47**, 204006 (2014).
 - [43] M. Klaiber, E. Yakaboylu, H. Bauke, K. Z. Hatsagortsyan, and C. H. Keitel, Phys. Rev. Lett. **110**, 153004 (2013).
 - [44] E. Yakaboylu, M. Klaiber, H. Bauke, K. Z. Hatsagortsyan, and C. H. Keitel, Phys. Rev. A **88**, 063421 (2013).
 - [45] D. M. Gitman, E. S. Fradkin, and S. M. Shvartsman, *Quantum Electrodynamics with Unstable Vacuum*, Springer Series in Nuclear and Particle Physics (Springer, Berlin, 1991).
 - [46] W. H. Furry, Phys. Rev. **81**, 115 (1951).
 - [47] This can be shown best in the gauge $A^\mu = (-Ex, 0, 0, -Bx)$ for the general constant crossed field case.
 - [48] A. I. Nikishov, Sov. Phys. JETP **30**, 660 (1970).
 - [49] H. R. Reiss, J. Math. Phys. **3**, 59 (1962).
 - [50] A. I. Nikishov, J. Russ. Laser Res. **6**, 619 (1985).
 - [51] V. S. Popov, V. P. Kuznetsov, and A. M. Perelomov, Sov. Phys. JETP **26**, 222 (1968).
 - [52] M. S. Marinov and V. S. Popov, Sov. J. Nucl. Phys. **15**, 702 (1972).
 - [53] W. Pauli, Helv. Phys. Acta **5**, 179 (1932).
 - [54] As we do not consider spin effects in this paper, the given actions do not include any spin or polarization terms.
 - [55] Using usual quantization rules, the photon will have no gauge, and therefore $K = k$. Furthermore, $P = p - eA$ and $Q = q + eA$, which gives $P + Q - K = p + q - k$.